Reliability-based topology optimization under random-field material model

Trung Pham, Christopher Hoyle

Here is the journal name manuscript No.
(will be inserted by the editor)

Reliability-based topology optimization under random-field material model

Trung Pham · Christopher Hoyle

Received: xx/xx/20xx / Accepted: date

Abstract This paper presents an algorithm for reliability-based topology optimization of linear elastic continua under random-field material model. The modelling random field is discretized into a small number of random variables, and then the interested output is estimated by a stochastic response surface. A single-loop inverse-reliability algorithm is applied to reduce computational cost of reliability analysis. Two common benchmark problems in literature are used for demonstration purposes. Different values of target reliability and ranges of Young's modulus are considered to investigate their effects on resulting optimized topologies. Lastly, Monte Carlo simulation tests the proposed algorithm for correctness and accuracy.

Keywords Continuum topology optimization · Material uncertainties · Structural reliability · Karhunen−Loève expansion · Stochastic response surface

1 Introduction

In structural design, geometrical and topological properties of the design have significant impacts on structural performance. Topology optimization (TO) has emerged as an effective method to optimize such properties, including size, shape, and connectivity of the design (Bendsøe and Sigmund, 2003). TO can identify designs with improved performance while using the least amount of material. However, deterministic inputs have often been assumed in research on TO, while most observable phenomena contain an inherent amount of uncertainty; in the analysis and design of engineering systems the presence of uncertainty has always induced an acute impact. Ignoring uncertainty may produce sub-optimal designs that perform poorly under random inputs. Among different sources of uncertainty, the material property is inherently random in space and can be modeled by a random field. Therefore, this paper proposes an algorithm for reliability-based topology optimization under a random-field material model. Specifically, the Karhunen−Loève expansion discretizes the modeling random field into a small number of random variables, and then the output of interest is estimated by the stochastic response surface method. The uncertainty in material property makes the problem constraints probabilistic, which will require a drastically different approach for the optimization problem. A single-loop algorithm called Sequential Optimization and Reliability Assessment (SORA) (Du and Chen, 2004) coupled with the performance measure approach (Tu et al., 1999) is used to reduce the computational cost of reliability analysis. The proposed algorithm is tested using two numerical examples, and finally verified by Monte Carlo simulation.

The layout of this paper is as follows. Section 2 is a literature review on the current state of the art providing background of uncertainty propagation, reliability analysis, and TO under uncertainty. Section 3 states the mathematical formulation of the deterministic and reliability-based topology optimization (RBTO) problem. This section also explains in detail our proposed solution for the RBTO problem. Numerical examples, including a simply supported beam and a L-shape beam, are done in section 4 with discussion of the results. Finally, the paper is concluded by findings and future work.

2 Background

Though there are different probability interpretations (Stanford Encyclopedia of Philosophy, 2018), in the context of

Trung Pham · Christopher Hoyle
School of Mechanical, Industrial & Manufacturing Engineering
Oregon State University
Corvallis, OR 97331–6001, USA
E-mail: chris.hoyle@oregonstate.edu

continuum mechanics the assumption of continuity over the entire domain makes it suitable to apply the so-called Kolmogorov's probability theory (Kolmogorov, 2018) to the problem of "design under uncertainty". Using such theory coupled with an appropriate solution method, uncertainty in TO has been tackled mainly in the settings of robust optimization (RO) and reliability-based optimization (RBO).

In RO the primary goal is to minimize the variability of outputs of interest due to uncertainty (Taguchi, 1986). This is usually archived by optimizing a weighted sum of mean and standard deviation of the objective function. This approach was implemented in a number of papers with various sources of uncertainty and solution methods: spatial variation of manufacturing error with Monte Carlo simulations (Schevenels et al., 2011); random-field truss material with a multi-objective approach (Richardson et al., 2015); random loading field and random material field with the level set method (Chen et al., 2010); material and geometric uncertainties with stochastic collocation methods and perturbation techniques (Lazarov et al., 2012a,b); misplacement of material and imperfect geometry (Jansen et al., 2013, 2015); Young's modulus of truss members with a perturbation method (Asadpoure et al., 2011); random-field material properties with a polynomial chaos expansion (Tootkaboni et al., 2012); geometric and material properties uncertainties with a stochastic perturbation method for frame structures (Changizi and Jalalpour, 2017); random loading field with stochastic collocation methods (Zhao et al., 2015b). A unified framework for robust topology optimization (RTO) was proposed in Richardson et al. (2016), while Zhao and Wang (2014) solved the RTO problem exploiting the linear elasticity of structure. Some authors (Jalalpour and Tootkaboni, 2016; Richardson et al., 2015) claimed that one weakness of the RO methodology is the seemingly arbitrary weighting factors, which actually reflect risk-taking attitude of designers (McIntire et al., 2014; Lewis et al., 2006).

In RBO some of the constraints become probabilistic, which need specialized methods to handle. The reason is that the probabilistic constraints are expressed by multiple integrals of the joint probability density function (PDF) of random variables, both of which are either practically impossible to obtain or very difficult to evaluate (Haldar and Mahadevan, 2000). Interested readers are advised to refer to Valdebenito and SchuÃńller (2010) for a complete review of RBO methods to overcome such difficulties. Within the scope of this paper, we only focus on the first-order reliability methods (FORM), the second-order reliability methods (SORM), the SORA method, and the stochastic response surface (SRS) method. FORM appeared early (Cornell, 1969) together with the concept of reliability index (Hasofer and Lind, 1974) to solve RBO problems. SORM (Fiessler et al., 1979) followed to improve accuracy of the FORM in case of highly nonlinear limit state functions and/or slow decay of the joint PDF. The main idea of FORM and SORM is to approximate the limit state functions using first-order and second-order Taylor series, respectively, at appropriate values (e.g., means) of random variables. This results in a double-loop optimization problem to find the most probable point (MPP). In the context of RBTO, directly solving the double-loop optimization problem has been shown in Maute and Frangopol (2003) for MEMS mechanisms with stochastic loading, boundary conditions as well as material properties; in Sato et al. (2018) for shape uncertainty; in Kang and Liu (2018) for geometric imperfections; in Mogami et al. (2006) for frame structures using system reliability under random-variable inputs; in Kang et al. (2004) for electromagnetic systems; and in Jung and Cho (2004) for geometrically nonlinear structures. This approach is prohibitively expensive and lacks robustness when a large number of random variables present (Schuëller et al., 2004). For this reason, single-loop approaches have been developed, in which, e.g., the Karush−Kuhn−Tucker (KKT) optimality conditions are utilized to avoid the inner loop. Both Nguyen et al. (2011) and Silva et al. (2010) used variants of the single-loop method in Liang et al. (2004) for component and system reliability-based TO. Kharmanda et al. (2004) is somewhat unique when using their own single-loop method (Kharmanda et al., 2002). Kogiso et al. (2010) applied the single-loop-single-vector method (Chen et al., 1997) for frame structures under random-variable loads and nonstrucutral mass. Another way to bypass the double-loop problem is the decoupling approaches (Valdebenito and SchuÃńller, 2010), in which reliability analysis results are used to facilitate the optimization loops. Among them, the SORA method is known for its simple implementation compared to the above single-loop methods, and efficiency with FORM (Du and Chen, 2004; Lopez and Beck, 2012). This method was employed for RBTO under random-variable inputs in Zhao et al. (2015a) and Zhao et al. (2016). Simulation techniques coupled with meta modeling or surrogate modeling have enjoyed considerable popularity within RBO community (Wang and Shan, 2007), but has received little attention in TO literature. In Patel and Choi (2012), reliability was assessed using probabilistic neural network classifier for truss structures under random Young's modulus.

To the best of our knowledge, Zhao et al. (2015a), Jalalpour and Tootkaboni (2016), and Keshavarzzadeh et al. (2017) are three papers closest to ours. However, random-field material model was not considered in Zhao et al. (2015a) and Keshavarzzadeh et al. (2017). Furthermore, several concerns can be identified from Keshavarzzadeh et al. (2017). One of the most important stages in their method is the approximations of failure probability and its sensitivity, which depend on Monte Carlo sampling, and the value of the parameter ϵ when replacing the Heaviside function with a smooth approximation (Keshavarzzadeh et al., 2016). Direct Monte Carlo sampling is well-known to have variability (Taflanidis and

Beck, 2008), meaning two independent runs are very likely to get different values of failure probability and its sensitivity which would obviously affect the optimization results. The parameter ϵ was chosen by a "recommendation" backed by observation only. Jalalpour and Tootkaboni (2016) assumed that the modeling random field has known marginal distribution, and random variability of Young's modulus is small in order to apply perturbation technique. Both of these assumptions clearly restrict the general applicability of their method. As described in the following sections, our proposed method considers random field uncertainty with the Karhunen−Loève (KL) expansion used to reduce the dimension of the random field. The KL expansion covers a large class of random field without any restrictions on random variability. In this way, we are able to use the FORM-based inverse reliability method within the SORA framework coupled with the stochastic response surface method to avoid the aforementioned drawbacks of direct Monte Carlo sampling.

3 Topology optimization under uncertainty

3.1 Deterministic topology optimization

This paper adopts a standard notation, which denotes matrices and vectors as bold upper and lower case letters respectively. The below formulation shows a density-based deterministic topology optimization:

$$\begin{aligned} \min_{\boldsymbol{\rho}} \quad & V(\boldsymbol{\rho}) = \boldsymbol{\nu}^T \boldsymbol{\rho} \\ \text{subject to} \quad & \mathbf{K}(\boldsymbol{\rho})\mathbf{u}(\boldsymbol{\rho}) = \mathbf{f}, \\ & u_i(\boldsymbol{\rho}) \le u_i^0,\ i = 1, 2, \ldots, m \\ & 0 < \rho_{\text{min}} \le \boldsymbol{\rho} \le 1. \end{aligned} \tag{1}$$

where $\boldsymbol{\rho}$ is the vector of deterministic finite-element densities; $V(\boldsymbol{\rho})$ is the total volume of the finite-element mesh; $\boldsymbol{\nu}$ is the vector of finite-element volumes for a unit density; $\mathbf{K}(\boldsymbol{\rho})$, $\mathbf{u}(\boldsymbol{\rho})$, and $\mathbf{f}$ are the stiffness matrix, the displacement vector, and the external load vector, respectively; $u_i(\boldsymbol{\rho})$ and $u_i^0, i = 1, 2, \ldots, m$, are the actual displacement and the maximum allowable displacement at the i^{th} degree of freedom. In the optimization problem (1), $\boldsymbol{\rho}$ is the design variables and $V(\boldsymbol{\rho})$ is the objective function. The first constraint expresses the equilibrium of the structure while the third constraint is a component-wise inequality, in which each density (design variable) must be between 1 and a lower limit (e.g., $\rho_{\text{min}} = 0.001$).

To promote manufacturing of the resulting structure, a black-and-white design is preferred. Hence, the Solid Isotropic Material with Penalization (SIMP) method (Bendsøe and Sigmund, 2003) is used to penalize the intermediate values. According to SIMP, the Young's modulus of each finite elements E_i is obtained as $E_i = \rho_i^p E_i^0$, where p is the penalization factor and E_i^0 is the initial value of the Young's modulus corresponding to unit density. The possible values of p were explained in Bendsøe and Sigmund (1999). Applying SIMP transforms the problem (1) into a nonlinear optimization problem, which can be solved effectively by many gradient-based algorithms. The Method of Moving Asymptotes (MMA) (Svanberg, 1987, 2002) is chosen in this paper due to its reliability to catch extremum in various settings of TO. Known problems with SIMP are checkerboarding, mesh dependence, and local minima (Sigmund and Petersson, 1998). Checkerboarding and mesh dependence can be prevented by mesh independent filtering methods (Sigmund, 2007). This paper uses the density filtering (Bruns and Tortorelli, 2001; Bourdin, 2001) as implemented in Andreassen et al. (2011). In the next section we will discuss the changes needed to integrate uncertainty into the optimization problem.

3.2 Reliability-based topology optimization

When uncertainty is introduced into the problem (1) in the form of a modeling random field $y(\omega, \mathbf{x})$, the second constraints have to be replaced as follows:

$$\begin{aligned} \min_{\boldsymbol{\rho}} \quad & V(\boldsymbol{\rho}) = \boldsymbol{\nu}^T \boldsymbol{\rho} \\ \text{s.t.} \quad & \mathbf{K}(\boldsymbol{\rho}, y)\mathbf{u}(\boldsymbol{\rho}, y) = \mathbf{f}, \\ & P_i[u_i^0 - u_i(\boldsymbol{\rho}, y) < 0] \le P_i^0,\ i = 1, 2 \ldots, m \\ & 0 < \rho_{\text{min}} \le \boldsymbol{\rho} \le 1. \end{aligned} \tag{2}$$

where $\mathbf{x} \in D \subset \mathbb{R}^d$ is coordinates of a point in a d-dimensional physical domain D, $\omega \in \Omega$ is an element of the sample space Ω, $P_i[\cdot]$ is the probability, P_i^0 is the target probability of the i^{th} constraint. The limit state function is defined as $g(\boldsymbol{\rho}, y) = u^0 - u(\boldsymbol{\rho}, y)$, so $g(\boldsymbol{\rho}, y) < 0$ means constraint violation or failure of the structure in (1) while $P_i[g_i(\boldsymbol{\rho}, y) < 0]$ shows the failure probability of the i^{th} constraint. The target probability P_i^0 is the upper bound of the failure probability P_i and often defined as $P_i^0 = \Phi(-\beta_i)$, where β_i is the reliability index and $\Phi(\cdot)$ is the standard normal cumulative distribution function.

Several complications arise when a RBO problem involves a random field. In many cases the considered random field is a infinite-dimensional set, which makes it extremely difficult to propagate uncertainty from input to output of a system if used directly. Instead, the random field usually has to be discretized or dimensionally reduced to a manageable order, which we will show in Sect. 3.2.1. The double-loop RBO problem can be very expensive to solve, which is considered in Sect. 3.2.2. The probabilistic constraint is often implicit and very hard to evaluate because of complex geometry of its domain, which becomes much easier and cheaper to compute if approximated by the stochastic response surface (SRS) method in Sect. 3.2.3. This section ends with a

thorough description of our proposed algorithm for a RBTO problem based on the above methods.

3.2.1 Karhunen−Loève expansion

A random field can be discretized by serveral methods including the Expansion Optimal Linear Estimator (Li and Der Kiureghian, 1993) and polynomial chaos expansion (Xiu, 2010; Ghanem and Spanos, 2003). Compared to others, the Karhunen−Loève (KL) expansion (Loève, 2017) is "the most effcient in terms of the number of random variables required for a given accuracy" (Sudret and Kiureghian, 2000). The KL expansion of a random field $y(\omega, \mathbf{x})$ is given as

$$y(\omega, \mathbf{x}) = E[\mathbf{x}] + \sum_{i=1}^{\infty} \sqrt{\lambda_i}\xi_i(\omega)e_i(\mathbf{x}) \tag{3}$$

where $E[\mathbf{x}]$ is the mean of the random field. The orthogonal eigenfunctions $e_i(\mathbf{x})$ and the corresponding eigenvalues λ_i are solutions of the following eigenvalue problem:

$$\int_D K(\mathbf{x}_1, \mathbf{x}_2)e_i(\mathbf{x})d\mathbf{x} = \lambda_i e_i(\mathbf{x}) \quad \mathbf{x}, \mathbf{x}_1, \mathbf{x}_2 \in D \tag{4}$$

where $K(\mathbf{x}_1, \mathbf{x}_2)$ is the covariance function of the random field

$$K(\mathbf{x}_1, \mathbf{x}_2) = E\left[y(\mathbf{x}_1)y(\mathbf{x}_2)\right] \quad \mathbf{x}_1, \mathbf{x}_2 \in D \tag{5}$$

The random variables $\xi_i(\omega)$ are uncorrelated and satisfy:

$$\begin{aligned} &E[\xi_i] = 0, E[\xi_i\xi_j] = \delta_{ij} \\ &\xi_i(\omega) = \frac{1}{\sqrt{\lambda_i}} \int_D \left(y(\omega, \mathbf{x}) - E[\mathbf{x}]\right) e_i(\mathbf{x})d\mathbf{x} \end{aligned} \tag{6}$$

where δ_{ij} is the Kronecker delta. The infinite series in (3) has to be truncated to use in practice. Based on the fact that the influence of higher order terms decays rapidly, only a few of the terms are needed to capture behavior of the random field with appropriate precision.

The KL expansion requires the solution of the eigenvalue problem (4), which is pretty straightforward in the case of a random process (1-dimensional random field) (Ray and Sahu, 2013). For the purpose of demonstration and without loss of generality, this paper in Sect. 4 exploits the separability of the covariance function of a 2-dimensional random field:

$$\begin{aligned} K(\mathbf{s}, \mathbf{t}) &= exp\left(\frac{-|s_1 - t_1|}{l_1} \times \frac{-|s_2 - t_2|}{l_2}\right) \\ &= exp\left(-\frac{|s_1 - t_1|}{l_1}\right) exp\left(-\frac{|s_2 - t_2|}{l_2}\right) \\ &\mathbf{s}, \mathbf{t} \in D \subset \mathbb{R}^2 \end{aligned} \tag{7}$$

where l_1 and l_2 are the correlation lengths in the two coordinate directions. This class of covariance function makes the eigenvalues and eigenfunctions separable in the sense that both are the product of their univariate counterparts (Wang, 2008).

3.2.2 Inverse reliability and SORA

The form of the probabilistic constraints in (2) is called the reliability index approach (RIA). However, according to Tu et al. (1999), the performance measure approach (PMA) provides better numerical stability and higher rate of convergence. Using the PMA, (2) is rewritten as

$$\begin{aligned} \min_{\boldsymbol{\rho}} \quad & V(\boldsymbol{\rho}) = \boldsymbol{\nu}^T\boldsymbol{\rho} \\ \text{s.t.} \quad & \mathbf{K}(\boldsymbol{\rho}, y)\mathbf{u}(\boldsymbol{\rho}, y) = \mathbf{f}, \\ & u_i^0 - u_i(\boldsymbol{\rho}, y) \geq 0,\ i = 1, 2 \ldots, m \\ & 0 < \rho_{\text{min}} \leq \boldsymbol{\rho} \leq 1. \end{aligned} \tag{8}$$

Solving the above problem requires a truncated KL expansion $y(\omega, \mathbf{x}) \approx y(\xi_i(\omega), \mathbf{x})$, FORM, and inverse reliability analysis. In order to apply FORM, the random vector $\boldsymbol{\Xi} = \{\xi_i\}$ is transformed into a vector of standard normal random variables $\boldsymbol{\Psi} = \{\psi_i\}$ using the Rosenblatt or the Nataf transformation $\boldsymbol{\Psi} = T(\boldsymbol{\Xi})$ or $\boldsymbol{\Xi} = T^{-1}(\boldsymbol{\Psi})$. Then, the most probable point (MPP) $\boldsymbol{\xi}_i^*$ in physical space or $\boldsymbol{\psi}_i^*$ in transformed space is obtained by inverse reliability analysis:

$$\begin{aligned} \min_{\boldsymbol{\psi}} \quad & g_i(\boldsymbol{\psi}) \\ \text{s.t.} \quad & \parallel \boldsymbol{\psi} \parallel = \beta_i. \end{aligned} \tag{9}$$

where $g_i(\boldsymbol{\psi})$ is the i^{th} limit state function. In this paper, the Matlab CODES toolbox (Missoum et al., 2015) is chosen to solve (9). Also, the SORA framework is adopted to decouple the double-loop structure of (8). In SORA, instead of nesting the optimization problem (9) within (8), it serializes (8) into a chain of loops of deterministic TO and inverse reliability analysis (Fig. 1). Each k^{th} loop starts with deterministic TO followed by inverse reliability analysis:

$$\begin{aligned} \min_{\boldsymbol{\rho}^k} \quad & V(\boldsymbol{\rho}^k) = \boldsymbol{\nu}^T\boldsymbol{\rho}^k \\ \text{s.t.} \quad & \mathbf{K}(\boldsymbol{\rho}, y)\mathbf{u}(\boldsymbol{\rho}, y) = \mathbf{f}, \\ & u_i^0 - u_i\left(\boldsymbol{\rho}^k, y(\boldsymbol{\xi}_i^{*(k-1)}, \mathbf{x})\right) \geq 0,\ i = 1, 2 \ldots, m \\ & 0 < \rho_{\text{min}} \leq \boldsymbol{\rho}^k \leq 1. \end{aligned} \tag{10}$$

where $\boldsymbol{\xi}_i^{*(k-1)}$ denotes the MPP in physical space of i^{th} limit state function in the $(k-1)^{th}$ loop. Solving (10) gives $\boldsymbol{\rho}^{*(k)}$, which is substituted into (9) to find the next MPP $\boldsymbol{\xi}_i^{*(k)}$ in the form of $\boldsymbol{\psi}_i^{*(k)}$:

$$\begin{aligned} \min_{\boldsymbol{\psi}} \quad & g_i(\boldsymbol{\rho}^{*(k)}, \boldsymbol{\psi}) \\ \text{s.t.} \quad & \parallel \boldsymbol{\psi} \parallel = \beta_i. \end{aligned} \tag{11}$$

The computational cost is saved by a significant reduction in the number of reliability analyses needed until both the deterministic TO and reliability analysis converge. One obvious

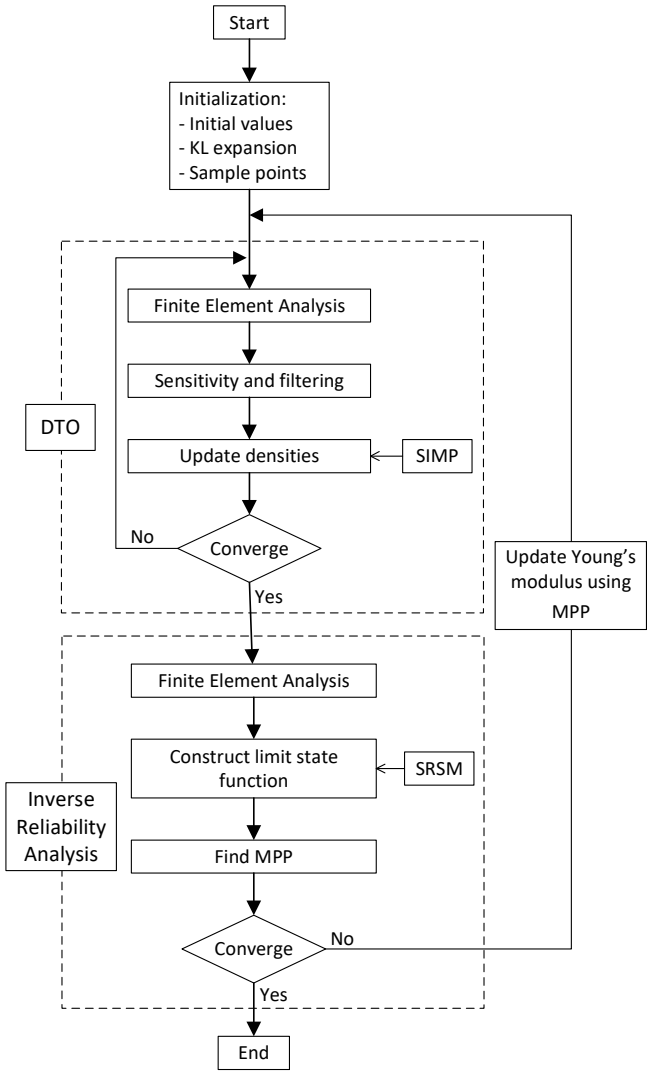

Fig. 1: SORA-based RBTO flowchart (Zhao et al., 2015a).

problem of the above scheme is that the final $\boldsymbol{\rho}^*$ may not be the same as in the double-loop setting, which is compensated for by shifting the random design variables in each loop (Yin and Chen, 2006). Since there is no random design variable (only random parameters) in the setting of this paper, no such modification is needed.

3.2.3 Stochastic response surface method

Considering random inputs, the propagated uncertainty in many cases makes it difficult to get an explicit expression of interested outputs, which blocks further progress, such as taking derivatives and optimization. The SRS method overcomes this problem by approximating the outputs by a polynomial chaos expansion (Xiu, 2010). The below formulations follows Huang and Kou (2007). The multidimensional Hermite polynomials of degree p are used in the SRS method and defined as:

$$H_p(\alpha_{i_1}, \alpha_{i_2}, \ldots, \alpha_{i_p}) = (-1)^p e^{\frac{1}{2}\boldsymbol{\alpha}^T\boldsymbol{\alpha}} \frac{\partial^p}{\partial\alpha_{i_1}, \partial\alpha_{i_2}, \ldots, \partial\alpha_{i_p}} e^{-\frac{1}{2}\boldsymbol{\alpha}^T\boldsymbol{\alpha}} \tag{12}$$

where $\boldsymbol{\alpha} = \{\alpha_{i_k}\}_{k=1}^{p}$ is a vector of standard normal random variables. The interested output z is estimated as follows:

$$z = a_0 + \sum_{i_1=1}^{n} a_{i_1} H_1(\alpha_{i_1}) + \sum_{i_1=1}^{n}\sum_{i_2=1}^{i_1} a_{i_1 i_2} H_2(\alpha_{i_1}, \alpha_{i_2}) + \sum_{i_1=1}^{n}\sum_{i_2=1}^{i_1}\sum_{i_3=1}^{i_2} a_{i_1 i_2 i_3} H_3(\alpha_{i_1}, \alpha_{i_2}, \alpha_{i_3}) + \ldots \tag{13}$$

where n is the number of standard normal random variables used in the expansion, and $a_0, a_{i_1}, a_{i_1 i_2}, a_{i_1 i_2 i_3}, \ldots$ are unknown coefficients. If $n = 2$ and $p = 3$, then the expansion (13) will become:

$$\begin{aligned} z(\alpha_{i_1}, \alpha_{i_2}) = \; & a_0 + a_1\alpha_{i_1} + a_2\alpha_{i_2} + a_3(\alpha_{i_1}^2 - 1) + a_4(\alpha_{i_2}^2 - 1) \\ & + a_5\alpha_{i_1}\alpha_{i_2} + a_6(\alpha_{i_1}^3 - 3\alpha_{i_1}) + a_7(\alpha_{i_2}^3 - 3\alpha_{i_2}) \\ & + a_8(\alpha_{i_1}\alpha_{i_2}^2 - \alpha_{i_1}) + a_9(\alpha_{i_1}^2\alpha_{i_2} - \alpha_{i_2}) \\ = \; & a_0 + \sum_{k=1}^{9} a_k \eta_{i_k} \end{aligned} \tag{14}$$

where $1, \eta_{i_1}, \eta_{i_2}, \ldots, \eta_{i_9}$ are Hermite polynomials. The ten unknown coefficients $a_0, a_1, \ldots, a_9$ are found by solving a system of linear equations using at least ten different realizations of $(\alpha_{i_1}, \alpha_{i_2})$. A stochastic response surface constructed with 17 collocation points was shown to be a very good approximation in Huang and Kou (2007), which will be used in this paper.

3.2.4 Solution algorithm

A step-by-step explanation of our solution algorithm (Fig. 1) is listed below:

1. Initialize the problem: finite element mesh; initial values of design variables, SIMP and optimization parameters; Karhunen−Loève (KL) expansion of random field; sample points for the stochastic response surface method (SRSM); etc.
2. Deterministic topology optimization (DTO): the SIMP method and the MMA are used to solve (10), which is deterministic because there is no random variable involved. To guarantee that the Young's modulus is physically meaningful (e.g., only positive values), it is modeled as in Lazarov et al. (2012a):

$$E(\mathbf{x}) = F^{-1} \circ \Phi\left[y(\omega, \mathbf{x})\right] \tag{15}$$

where $\Phi[\cdot]$ is the standard normal cumulative distribution function (CDF) and F^{-1} is the inverse of a prescribed CDF. The uniform distribution is chosen in this paper resulting in

$$E(\mathbf{x}) = a + (b-a)\Phi\left[y(\omega, \mathbf{x})\right] \tag{16}$$

where a and b are the two bounds of the distribution. Two other physically admissible distributions are the log-normal and the beta distribution, which can replace the uniform distribution in (15) with trivial effort.

3. Inverse reliability analysis (IRA): the optimum values of design variables (densities) found in the previous stage and the sample points are used to construct response surfaces of the probabilistic constraints, which in turn are utilized in (11) to find the most probable point (MPP). Based on convergence conditions, the algorithm may stop or a new loop is requested with updated Young's modulus using the MPP.

4 Results

In this section two common benchmark problems (the MBB and the L-shaped beam) are used to test our proposed algorithm with three values of target reliability and four different parameter tuples of the uniform distribution in (16). The optimization results are then verified by Monte Carlo simulations. For simplicity, all quantities are given dimensionless.

The two numerical examples below share some common implementation settings. Square, linear plane stress element is employed in both examples, which has unit side length and thickness, and is made of isotropic linear elastic material with Poisson's ratio $\nu = 0.3$. The material Young's modulus is assumed to be a centered mean-square Gaussian random field with known covariance function as in (7). Under such assumption, the KL expansion results in a series of independent standard normal random variables (Alexanderian, 2015). The correlation length are chosen as $l_1 = l_2 = 0.6$, and the truncated KL expansion contains the first two eigenvalues and eigenfunctions. The CODES toolbox provides a wide range of optimization algorithms, among which the Hybrid Mean Value (HMV) method is chosen due to its efficiency (Youn et al., 2003). The three values of target reliability are $\{2.0, 2.5, 3.0\}$ while the four parameter tuples are $(a, b) = \{(1, 1.1), (1, 1.3), (1, 1.5), (1, 1.7)\}$. The MMA is the optimizer running on design variables in DTO until convergence criterion, e.g., maximum difference of design variables of two consecutive iterations $(d_{\max} = 0.001)$, is satisfied. The IRA stage is considered converged if maximum difference of the MPPs of the previous and current loop is smaller than 0.001, and the number of iterations is smaller then 20. In SIMP, the minimum length scale $r_{\min} = 1.5$ and penalization factor $p = 3$ are employed. For verification,

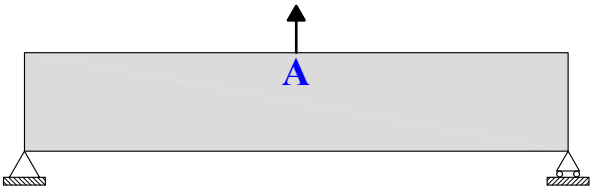

Fig. 2: The MBB beam

50000 Monte Carlo simulations (MCS) are run to calculate the failure probabilities and the statistical moments, which are compared with the expected failure probabilities computed from the three reliability levels, and the SRSM-based results.

4.1 The MBB beam

Consider the simply supported, two-dimensional domain in Fig. 2. It is subject to an unit vertical load at the midpoint of its top edge and meshed into 120×20 elements. For the purpose of this paper, its volume is minimized under a constraint on the displacement of the load application point. The maximum allowable vertical displacement of the load application point (point A in Fig. 2) is given as $u^0 = 170$. This value is picked up for demonstration purpose: volume fraction of RBTO results, i.e., ratio of optimized volume to that of initial domain, will be in the range of $(0.4, 0.6)$ facilitating visual inspection; any reasonable values should work. Only one half of the domain (60×20 elements) needs to be optimized due to its symmetry.

For comparison with RBTO results, the deterministic topology optimization (DTO) is performed with the Young's modulus equal to $\{1.05, 1.15, 1.25, 1.35\}$, which are the means of the corresponding uniform distributions in Table 1. Table 2 shows DTO results of the MBB beam found by solving (1), and their volume fractions. Next, the proposed algorithm is run with different values of target reliability and material parameters resulting in 12 optimized designs as shown in Table 1. To verify our proposed algorithm, the results in Table 1 are used in the MCS and SRSM. The mean μ and the standard deviation σ of vertical displacement of point A, and the failure probabilities P_f of the constraint in (2) are aggregated in Table 3 from those simulations. Finally, the cumulative distribution function (CDF) of vertical displacement of point A is plotted. Because the CDF plots constructed from the MCS and SRSM are very close to each other for every combination of reliability levels and material parameters and no additional conclusion can be drawn by including all of them, only one CDF plot in the case of $\beta = 2.5$ and $(a, b) = (1, 1.5)$ is shown in Fig. 4b. Also, the last 10 points of the simulations, which belong to the tail of the CDF where failure probabilities are determined, are displayed in

Table 1: The MBB beam: RBTO results

(a,b)	$(1,1.1)$	$(1,1.3)$	$(1,1.5)$	$(1,1.7)$
$\beta=2$				
$\beta=2.5$				
$\beta=3$				

Table 2: The MBB beam: DTO results

E	1.05	1.15	1.25	1.35
DTO				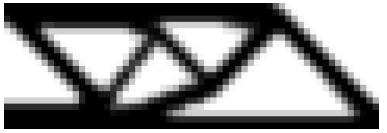
Volume fraction	0.5961	0.5464	0.5051	0.4693

Table 3: The MBB beam: MCS, SRSM, and volume fraction

				MCS			SRSM	
β	Expected P_f	(a, b)	Volume fraction	μ	σ	P_f	μ	σ
2	0.02275	$(1, 1.1)$	0.5972	169.751	0.1238	0.02192	169.751	0.1238
		$(1, 1.3)$	0.5452	169.318	0.3386	0.02242	169.318	0.3386
		$(1, 1.5)$	0.5070	168.952	0.5196	0.02242	168.952	0.5196
		$(1, 1.7)$	0.4732	168.654	0.6665	0.02276	168.654	0.6665
2.5	0.00620	$(1, 1.1)$	0.5974	169.689	0.1236	0.00554	169.689	0.1236
		$(1, 1.3)$	0.5457	169.147	0.3381	0.00564	169.147	0.3381
		$(1, 1.5)$	0.5074	168.682	0.5209	0.00578	168.682	0.5209
		$(1, 1.7)$	0.4740	168.315	0.6643	0.00584	168.315	0.6643
3	0.001349	$(1, 1.1)$	0.5977	169.628	0.1232	0.001320	169.628	0.1232
		$(1, 1.3)$	0.5463	168.976	0.3376	0.001340	168.976	0.3376
		$(1, 1.5)$	0.5081	168.411	0.5218	0.001380	168.411	0.5218
		$(1, 1.7)$	0.4742	167.970	0.6640	0.001360	167.970	0.6640

Fig. 4a to aid visual inspection. A number of conclusions and observations from this example will be discussed in Sect. 5.

4.2 The L-shaped beam

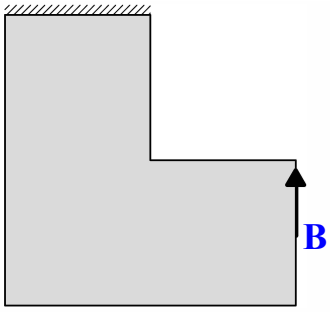

Fig. 3: The L-shaped beam

The second numerical example to illustrate our proposed algorithm is the L-shaped beam as shown in Fig. 3. The beam is fixed on its topmost edge and subject to a unit vertical load at the midpoint of the rightmost edge. As in the previous example, the volume of the beam is minimized while the probabilistic constraint is to limit the vertical displacement of the load application point (point B in Fig. 3). The maximum allowable vertical displacement of point B is chosen as $u^0 = 100$. Again, this number is only to make sure the results are visually friendly. The design domain is discretized using a 60×60 mesh of finite elements. One quarter of the mesh is removed to make the domain L-shaped by setting the element densities in this region to 0.001 before proceeding to the next loop.

Compared to the MBB beam, this example uses a larger number of elements (3600 vs. 1200) resulting in much more time to finish the MCS. On the same machine, it took approximately 15 minutes to produce one row in Table 3 but nearly 2.5 hours for the L-shaped beam. Furthermore, after examining the results, almost the same trends as in the previous example are observed. Thus, we decide to run MCS for only six cases as shown in Table 6. Those cases are the combinations of $\beta = \{2, 3\}$ and $(a, b) = \{(1, 1.3), (1, 1.5), (1, 1.7)\}$. The failure probabilities of the vertical displacement constraint at point B, and the statistical moments of that point's vertical displacement are calculated using both the MCS and SRSM in Table 6. Table 4 and 5 show the RBTO and DTO results of the L-shaped beam, respectively. Lastly, the CDF of point B vertical displacement and its last 10 points are displayed respectively in Fig. 5b and 5a. Several insights and discussions are provided in the next section.

5 Discussions

The results from the two examples are studied in this section for comparison, verification, and insights.

Visually, it is hard for human eyes to detect any differences between the RBTO results and the corresponding DTO results using the mean values of the Young's modulus. We are also not aware of any tools to find such differences, at least in the field of topology optimization, and hence believe this would be a research direction of great utility, especially when considering uncertainty and different material models.

Table 4: The L-shaped beam: RBTO results

(a,b)	$(1,1.3)$	$(1,1.5)$	$(1,1.7)$
$\beta=2$			
$\beta=3$			

Table 5: The L-shaped beam: DTO results

E	1.15	1.25	1.35
DTO	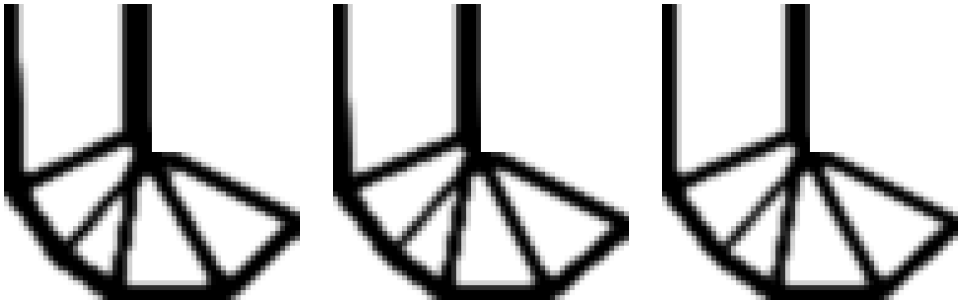		
Volume fraction	0.3542	0.3281	0.3097

Table 6: The L-shaped beam: MCS, SRSM, and volume fraction

				MCS			SRSM	
β	Expected P_f	(a,b)	Volume fraction	μ	σ	P_f	μ	σ
2	0.02275	$(1,1.3)$	0.3552	99.628	0.1844	0.02174	99.628	0.1844
		$(1,1.5)$	0.3291	99.420	0.2873	0.02198	99.420	0.2873
		$(1,1.7)$	0.3117	99.254	0.3688	0.02200	99.254	0.3688
3	0.001349	$(1,1.3)$	0.3557	99.444	0.1832	0.001140	99.444	0.1832
		$(1,1.5)$	0.3295	99.127	0.2867	0.001120	99.127	0.2867
		$(1,1.7)$	0.3153	98.881	0.3664	0.001120	98.881	0.3664

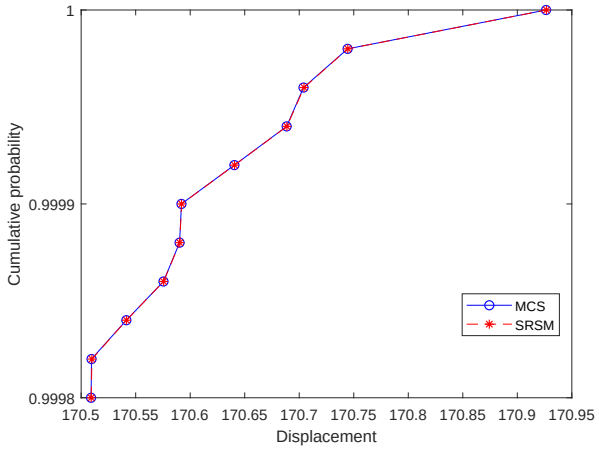

(a) The last 10 points of the CDF

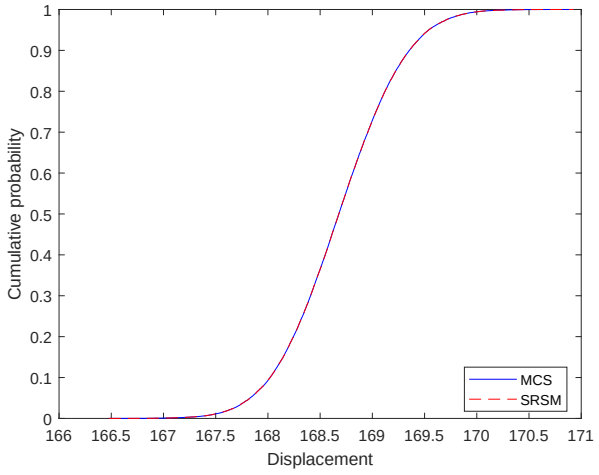

(b) The full CDF plot

Fig. 4: The MBB beam: CDF plot for $\beta = 2.5$ and $(a, b) = (1, 1.5)$

In the meantime, to compare those results qualitatively, readers can compile them column-wise (i.e., $(a, b) = (1, 1.5)$ in Table 1 and $E = 1.25$ in Table 2) into short animations, which are not possible to show in here. It turns out that there are material redistribution among most of the results, thickening or thinning of features, and even removal or addition of features (i.e., $(a, b) = (1, 1.3)$ in Table 1 vs. $E = 1.15$ in Table 2; $(a, b) = (1, 1.7)$ in Table 4 vs. $E = 1.35$ in Table 5).

The optimized designs together with the numbers in Table 3 and 6 reveal several trends:

1. For the same reliability target, increasing variability of the material property (i.e., bigger b in (a, b)) will decrease the volume fraction. This is reflected in thinner features or complete removal of features. For example, the features of the four designs in the first row of Table 1 become thinner when increasing the range, making their "inner" spaces sparser. Smaller features can be translated into smaller cross section (i.e., of beam or truss member). This trend is also visible if ones look at the DTO results, which are found using the mean of the range (a, b). If MCS are run on the DTO results, the failure probabilities will be around 0.5, which is equivalent to $\beta = 0$. This trend can be explained by the fact that the Young's modulus in the two examples is modelled by the uniform distribution, in which all intervals of the same length on the distribution's support have the same probability, and displacement is smaller with bigger value of the Young's modulus. Also, the mean and standard deviation of the vertical displacement have opposite trends: the mean decreases while the standard deviation becomes bigger. This is obviously caused by the increasing range while keeping the maximum allowable displacement u^0 constant.
2. For the same range, a higher reliability target will increase the volume fraction. The changes in most cases are pretty small, leading to hard-to-detect differences in the optimized designs. However, such small changes achieve significantly distinct failure probabilities if viewing the second column of Table 3 and 6. Possibly smaller failure probability enforces tighter bounds on the vertical displacement (i.e., both the mean and standard deviation becomes smaller), which in turn requires a volume increment.
3. The failure probabilities computed by the MCS (the 7^{th} columns in Table 3 and 6) in most cases are smaller than the corresponding expected values (the 2^{nd} columns), which proves the correctness of our proposed algorithm. However, there are three outliers in Table 3 ($\beta = 2$ and $(a, b) = (1, 1.7)$; $\beta = 3$ and $(a, b) = \{(1, 1.5), (1, 1.7)\}$). Those values are somewhat expected. First, there are many levels of approximation in our algorithm from the KL expansion to inverse reliability analysis and the SRSM, which accumulates error in the final results. Second, the random data points used in the MCS, which are generated by Latin hypercube sampling, are scattered uniformly over the whole distribution of the vertical displacement. The results would be much more accurate if there are more data points in the tail of the distribution, which usually has very small probability and where failure happens (e.g., using importance sampling). Third, the pseudorandom number generator in Matlab works by taking an initial seed, which is 0 for the results in Table 3 and 6, and then generating a deterministic sequence of numbers. Different seeds produce different sequences resulting in slightly different probabilities. It is quite likely that for the seed we chose, an "unfavorable" sequence is accompanied leading to those outliers. Based on the above arguments, we are confident that our algorithm is working correctly.

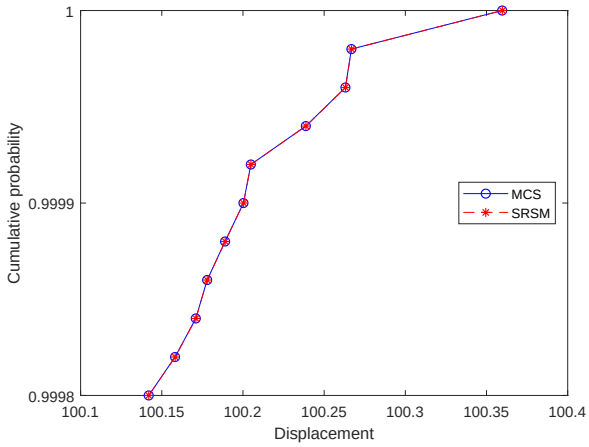

(a) The last 10 points of the CDF

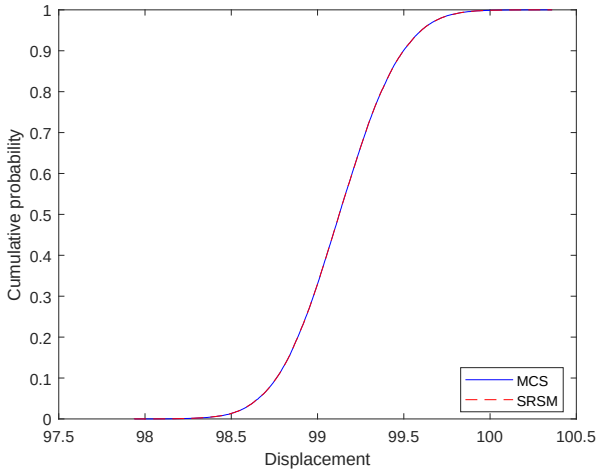

(b) The full CDF plot

Fig. 5: The L-shaped beam: CDF plot for $\beta = 3$ and $(a, b) = (1, 1.5)$

4. The MCS results in all cases agree well with the SRSM ones. From our observation, it is only possible to see the difference in the mean and standard deviation with 6 or more significant figures. Because of such small difference, the full CDF plots of the MCS and SRSM in Fig. 4b and 5b, as well as the last 10 points of those CDFs in Fig. 4a and 5a are almost indistinguishable. Thus, in the settings of out algorithm the SRSM works well and can be a strong, much cheaper alternative to the MCS.

6 Conclusions

In this work, we have presented a comprehensive approach to reliability-based design optimization considering random field uncertainty, specifically for application to topology optimization. The approach follows the Sequential Optimization and Reliability Assessment (SORA) approach formulated for random variable uncertainty, but extends the approach to consider random field uncertainty enabled using a Karhunen−Loève expansion and stochastic response surface. We have demonstrated the approach on two simple design examples and have shown that our framework is an efficient method to reliability-based design within a topology optimization approach to structural design. We have validated the approach by comparing the results from the SORA method to a Monte Carlo simulation.

The proposed approach is a first step to a comprehensive approach for design for additive manufacturing, or 3-D printing. Additive manufacturing approaches can lead to uncertainty in material properties, such as the modulus of elasticity, since the material is generally deposited in a sequential fashion. This material uncertainty can be represented as random field uncertainty as we have presented in this paper. Future work towards realizing topology optimization as a comprehensive approach to design for additive manufacturing includes several additional research directions. In general, many additive manufacturing processes deposit material in a layered pattern, so consideration of material anisotropy, in addition to material uncertainty, should be explored as a key feature of topology optimization design approach. Additionally, many additive manufacturing applications use polymeric materials which do not follow linear elastic material assumptions, but rather are better modeled assuming hyperelastic or viscoelastic material assumptions. Inclusion of material non-linearly may influence the design resulting from the TO process. Also, while we have considered uncertainty in the optimization constraints, leading to reliability-based design optimization, one should also consider uncertainty in the optimization objective function, leading to robust reliability based design optimization. In terms of validation, application of the proposed approach to more realistic design cases should be conducted. The simple examples in this paper were chosen to best illustrate the proposed SORA approach to topology optimization; however, design cases such as the design of airless tires, or tweels, should be conducted to better understand how the introduction of material uncertainty influences the resulting design.

Replication of Results
Matlab code for the two examples available at the Design Engineering Lab Github site `https://github.com/DesignEngrLab` in the project titled **RBTO**.

Compliance with Ethical Standards
The authors declare they have no conflict of interest.

Acknowledgements The first author would like to thank the Vietnam Education Foundation (VEF) for their financial support through the VEF fellowship, and Prof. Krister Svanberg for his assistance on the MMA code.

References

Alexanderian A (2015) A brief note on the Karhunen-Loève expansion

Andreassen E, Clausen A, Schevenels M, Lazarov BS, Sigmund O (2011) Efficient topology optimization in MATLAB using 88 lines of code. Structural and Multidisciplinary Optimization 43(1):1–16, DOI 10.1007/s00158-010-0594-7

Asadpoure A, Tootkaboni M, Guest JK (2011) Robust topology optimization of structures with uncertainties in stiffness − Application to truss structures. Computers & Structures 89(11-12):1131–1141, DOI 10.1016/j.compstruc.2010.11.004

Bendsøe MP, Sigmund O (1999) Material interpolation schemes in topology optimization. Archive of Applied Mechanics (Ingenieur Archiv) 69(9-10):635–654, DOI 10.1007/s004190050248

Bendsøe MP, Sigmund O (2003) Topology optimization: theory, methods, and applications. Springer, Berlin ; New York

Bourdin B (2001) Filters in topology optimization. International Journal for Numerical Methods in Engineering 50(9):2143–2158, DOI 10.1002/nme.116

Bruns TE, Tortorelli DA (2001) Topology optimization of non-linear elastic structures and compliant mechanisms. Computer Methods in Applied Mechanics and Engineering 190(26-27):3443–3459, DOI 10.1016/S0045-7825(00)00278-4

Changizi N, Jalalpour M (2017) Robust topology optimization of frame structures under geometric or material properties uncertainties. Structural and Multidisciplinary Optimization 56(4):791–807, DOI 10.1007/s00158-017-1686-4

Chen S, Chen W, Lee S (2010) Level set based robust shape and topology optimization under random field uncertainties. Structural and Multidisciplinary Optimization 41(4):507–524, DOI 10.1007/s00158-009-0449-2

Chen X, Hasselman T, Neill D, Chen X, Hasselman T, Neill D (1997) Reliability based structural design optimization for practical applications. In: 38th Structures, Structural Dynamics, and Materials Conference, American Institute of Aeronautics and Astronautics, Kissimmee,FL,U.S.A., DOI 10.2514/6.1997-1403

Cornell C (1969) A probability-based structural code. ACI Journal Proceedings 66(12), DOI 10.14359/7446

Du X, Chen W (2004) Sequential Optimization and Reliability Assessment Method for Efficient Probabilistic Design. Journal of Mechanical Design 126(2):225, DOI 10.1115/1.1649968

Fiessler B, Neumann H, Rackwitz R (1979) Quadratic limit states in structural reliability. Journal of Engineering Mechanics Division 105(4):661–676

Ghanem R, Spanos P (2003) Stochastic Finite Elements: A Spectral Approach. Civil, Mechanical and Other Engineering Series, Dover Publications

Haldar A, Mahadevan S (2000) Probability, reliability, and statistical methods in engineering design. John Wiley

Hasofer AM, Lind NC (1974) Exact and invariant second moment code format. Journal of Engineering Mechanics Division 100(EM1):111–121

Huang S, Kou X (2007) An extended stochastic response surface method for random field problems. Acta Mechanica Sinica 23(4):445–450, DOI 10.1007/s10409-007-0090-5

Jalalpour M, Tootkaboni M (2016) An efficient approach to reliability-based topology optimization for continua under material uncertainty. Structural and Multidisciplinary Optimization 53(4):759–772, DOI 10.1007/s00158-015-1360-7

Jansen M, Lombaert G, Diehl M, Lazarov BS, Sigmund O, Schevenels M (2013) Robust topology optimization accounting for misplacement of material. Structural and Multidisciplinary Optimization 47(3):317–333, DOI 10.1007/s00158-012-0835-z

Jansen M, Lombaert G, Schevenels M (2015) Robust topology optimization of structures with imperfect geometry based on geometric nonlinear analysis. Computer Methods in Applied Mechanics and Engineering 285:452–467, DOI 10.1016/j.cma.2014.11.028

Jung HS, Cho S (2004) Reliability-based topology optimization of geometrically nonlinear structures with loading and material uncertainties. Finite Elements in Analysis and Design 41(3):311–331, DOI 10.1016/j.finel.2004.06.002

Kang J, Kim C, Wang S (2004) Reliability-based topology optimization for electromagnetic systems. COMPEL - The international journal for computation and mathematics in electrical and electronic engineering 23(3):715–723, DOI 10.1108/03321640410540647

Kang Z, Liu P (2018) Reliability-based topology optimization against geometric imperfections with random threshold model. International Journal for Numerical Methods in Engineering 115(1):99–116, DOI 10.1002/nme.5797

Keshavarzzadeh V, Meidani H, Tortorelli DA (2016) Gradient based design optimization under uncertainty via stochastic expansion methods. Computer Methods in Applied Mechanics and Engineering 306:47–76, DOI 10.1016/j.cma.2016.03.046

Keshavarzzadeh V, Fernandez F, Tortorelli DA (2017) Topology optimization under uncertainty via non-intrusive polynomial chaos expansion. Computer Methods in Applied Mechanics and Engineering 318:120–147, DOI 10.1016/j.cma.2017.01.019

Kharmanda G, Mohamed A, Lemaire M (2002) Efficient reliability-based design optimization using a hybrid space with application to finite element analysis. Structural and Multidisciplinary Optimization 24(3):233–245, DOI 10.1007/s00158-002-0233-z

Kharmanda G, Olhoff N, Mohamed A, Lemaire M (2004) Reliability-based topology optimization. Structural and Multidisciplinary Optimization 26(5):295–307, DOI 10.1007/s00158-003-0322-7

Kogiso N, Hirano Y, Nishiwaki S, Izui K, Yoshimura M, Min S (2010) Reliability-Based Topology Optimization of Frame Structures for Multiple Criteria Using SLSV Method. Journal of Computational Science and Technology 4(3):172–184, DOI 10.1299/jcst.4.172

Kolmogorov AN (2018) Foundations of the Theory of Probability, Second English Edition. Dover Publications, Newburyport

Lazarov BS, Schevenels M, Sigmund O (2012a) Topology optimization considering material and geometric uncertainties using stochastic collocation methods. Structural and Multidisciplinary Optimization 46(4):597–612, DOI 10.1007/s00158-012-0791-7

Lazarov BS, Schevenels M, Sigmund O (2012b) Topology optimization with geometric uncertainties by perturbation techniques. International Journal for Numerical Methods in Engineering 90(11):1321–1336, DOI 10.1002/nme.3361

Lewis K, Chen W, Schmidt L (2006) Decision Making in Engineering Design. ASME Press, New York

Li C, Der Kiureghian A (1993) Optimal Discretization of Random Fields. Journal of Engineering Mechanics 119(6):1136–1154, DOI 10.1061/(ASCE)0733-9399(1993)119:6(1136)

Liang J, Mourelatos ZP, Tu J (2004) A Single-Loop Method for Reliability-Based Design Optimization. In: Volume 1: 30th Design Automation Conference, ASME, Salt Lake City, Utah, USA, vol 2004, pp 419–430, DOI 10.1115/DETC2004-57255

Loève M (2017) Probability Theory: Third Edition. Dover Books on Mathematics, Dover Publications

Lopez RH, Beck AT (2012) Reliability-based design optimization strategies based on FORM: a review. Journal of the Brazilian Society of Mechanical Sciences and Engineering 34(4):506–514, DOI 10.1590/S1678-58782012000400012

Maute K, Frangopol DM (2003) Reliability-based design of MEMS mechanisms by topology optimization. Computers & Structures 81(8-11):813–824, DOI 10.1016/S0045-7949(03)00008-7

McIntire MG, Vasylkivska V, Hoyle C, Gibson N (2014) Applying robust design optimization to large systems. In: ASME 2014 International Design Engineering Technical Conferences and Computers and Information in Engineering Conference, Buffalo, NY, pp V02BT03A054–V02BT03A054

Missoum S, Lacaze S, Boroson E, Jiang P (2015) CODES Toolbox. Computational Optimal Design of Engineering Systems Laboratory. University of Arizona

Mogami K, Nishiwaki S, Izui K, Yoshimura M, Kogiso N (2006) Reliability-based structural optimization of frame structures for multiple failure criteria using topology optimization techniques. Structural and Multidisciplinary Optimization 32(4):299–311, DOI 10.1007/s00158-006-0039-5

Nguyen TH, Song J, Paulino GH (2011) Single-loop system reliability-based topology optimization considering statistical dependence between limit-states. Structural and Multidisciplinary Optimization 44(5):593–611, DOI 10.1007/s00158-011-0669-0

Patel J, Choi SK (2012) Classification approach for reliability-based topology optimization using probabilistic neural networks. Structural and Multidisciplinary Optimization 45(4):529–543, DOI 10.1007/s00158-011-0711-2

Ray SS, Sahu PK (2013) Numerical Methods for Solving Fredholm Integral Equations of Second Kind. Abstract and Applied Analysis 2013:1–17, DOI 10.1155/2013/426916

Richardson J, Coelho RF, Adriaenssens S (2016) A unified stochastic framework for robust topology optimization of continuum and truss-like structures. Engineering Optimization 48(2):334–350, DOI 10.1080/0305215X.2015.1011152

Richardson JN, Filomeno Coelho R, Adriaenssens S (2015) Robust topology optimization of truss structures with random loading and material properties: A multiobjective perspective. Computers & Structures 154:41–47, DOI 10.1016/j.compstruc.2015.03.011

Sato Y, Izui K, Yamada T, Nishiwaki S, Ito M, Kogiso N (2018) Reliability-based topology optimization under shape uncertainty modeled in Eulerian description. Structural and Multidisciplinary Optimization DOI 10.1007/s00158-018-2051-y

Schevenels M, Lazarov B, Sigmund O (2011) Robust topology optimization accounting for spatially varying manufacturing errors. Computer Methods in Applied Mechanics and Engineering 200(49-52):3613–3627, DOI 10.1016/j.cma.2011.08.006

Schuëller G, Pradlwarter H, Koutsourelakis P (2004) A critical appraisal of reliability estimation procedures for high dimensions. Probabilistic Engineering Mechanics 19(4):463–474, DOI 10.1016/j.probengmech.2004.05.004

Sigmund O (2007) Morphology-based black and white filters for topology optimization. Structural and Multidisciplinary Optimization 33(4-5):401–424, DOI 10.1007/s00158-006-0087-x

Sigmund O, Petersson J (1998) Numerical instabilities in topology optimization: A survey on procedures dealing with checkerboards, mesh-dependencies and local minima. Structural Optimization 16(1):68–75, DOI 10.1007/BF01214002

Silva M, Tortorelli DA, Norato JA, Ha C, Bae HR (2010) Component and system reliability-based topology optimization using a single-loop method. Structural and Multidisciplinary Optimization 41(1):87–106, DOI 10.1007/s00158-009-0401-5

Stanford Encyclopedia of Philosophy (2018) Interpretations of probability. URL `https://plato.stanford.edu/entries/probability-interpret/`

Sudret B, Kiureghian AD (2000) Stochastic Finite Element Methods and Reliability: A State-of-the-Art Report (Report No. UCB/SEMM-2000/08). Department of Civil and Environmental Engineering, University of California, Berkeley

Svanberg K (1987) The method of moving asymptotesâĂŤa new method for structural optimization. International Journal for Numerical Methods in Engineering 24(2):359–373, DOI 10.1002/nme.1620240207

Svanberg K (2002) A Class of Globally Convergent Optimization Methods Based on Conservative Convex Separable Approximations. SIAM Journal on Optimization 12(2):555–573, DOI 10.1137/S1052623499362822

Taflanidis AA, Beck JL (2008) An efficient framework for optimal robust stochastic system design using stochastic simulation. Computer Methods in Applied Mechanics and Engineering 198(1):88–101, DOI 10.1016/j.cma.2008.03.029

Taguchi G (1986) Introduction to quality engineering: designing quality into products and processes. Distributed by the American Supplier Institute, Inc., Dearborn, MI

Tootkaboni M, Asadpoure A, Guest JK (2012) Topology optimization of continuum structures under uncertainty − A Polynomial Chaos approach. Computer Methods in Applied Mechanics and Engineering 201-204:263–275, DOI 10.1016/j.cma.2011.09.009

Tu J, Choi KK, Park YH (1999) A New Study on Reliability-Based Design Optimization. Journal of Mechanical Design 121(4):557, DOI 10.1115/1.2829499

Valdebenito MA, SchuÃńller GI (2010) A survey on approaches for reliability-based optimization. Structural and Multidisciplinary Optimization 42(5):645–663, DOI 10.1007/s00158-010-0518-6

Wang GG, Shan S (2007) Review of Metamodeling Techniques in Support of Engineering Design Optimization. Journal of Mechanical Design 129(4):370, DOI 10.1115/1.2429697

Wang L (2008) Karhunen−Loève Expansions and their Applications. PhD thesis, London School of Economics and Political Science

Xiu D (2010) Numerical Methods for Stochastic Computations: A Spectral Method Approach. Princeton University Press

Yin X, Chen W (2006) Enhanced sequential optimization and reliability assessment method for probabilistic optimization with varying design variance. Structure and Infrastructure Engineering 2(3-4):261–275, DOI 10.1080/15732470600590317

Youn BD, Choi KK, Park YH (2003) Hybrid Analysis Method for Reliability-Based Design Optimization. Journal of Mechanical Design 125(2):221, DOI 10.1115/1.1561042

Zhao J, Wang C (2014) Robust topology optimization under loading uncertainty based on linear elastic theory and orthogonal diagonalization of symmetric matrices. Computer Methods in Applied Mechanics and Engineering 273:204–218, DOI 10.1016/j.cma.2014.01.018

Zhao Q, Chen X, Ma ZD, Lin Y (2015a) Reliability-Based Topology Optimization Using Stochastic Response Surface Method with Sparse Grid Design. Mathematical Problems in Engineering 2015:1–13, DOI 10.1155/2015/487686

Zhao Q, Chen X, Ma ZD, Lin Y (2015b) Robust Topology Optimization Based on Stochastic Collocation Methods under Loading Uncertainties. Mathematical Problems in Engineering 2015:1–14, DOI 10.1155/2015/580980

Zhao Q, Chen X, Ma Z, Lin Y (2016) A Comparison of Deterministic, Reliability-Based Topology Optimization under Uncertainties. Acta Mechanica Solida Sinica 29(1):31–45, DOI 10.1016/S0894-9166(16)60005-8